(MURC-Tg) developed cardiomyocyte hypertrophy at 5 wk of age (11). These results suggest that MURC/Cavin-4 is involved in α1-AR signaling and cardiac hypertrophy.

In the present study, we manipulated MURC/Cavin-4 expression to investigate the role of MURC/Cavin-4 in caveolar morphology and α1-AR–induced cardiac hypertrophy. Overexpression and deletion of MURC/Cavin-4 showed the roles of MURC/Cavin-4 in the caveolar morphology of cardiomyocytes. Furthermore, we found that MURC/Cavin-4 facilitated ERK1/2 recruitment to caveolae and ERK activation in α1-AR–induced concentric cardiomyocyte hypertrophy.

Results

MURC/Cavin-4 Forms Caveolin–Cavin Complexes in the Caveolae and T Tubules and Modulates Caveolar Morphology in Cardiomyocytes. To reveal the functional significance of MURC/Cavin-4 as a caveolar component in cardiomyocytes, we examined the association of MURC/Cavin-4 with other cavins and caveolins. Expression plasmids encoding MURC/Cavin-4, Cav-3, and PTRF/Cavin-1 were transfected into CV-1 (simian) in origin, and carrying the SV40 genetic material (COS) cells, a fibroblast-like cell line derived from monkey kidney tissue. Immunoblot analysis showed that MURC/Cavin-4 was coimmunoprecipitated with Cav-3 and PTRF/Cavin-1 (Fig. S1 *A* and *B*). MURC-HA and Cav-3-T7 expressions were not reduced in supernatants immunoprecipitated by anti-T7 and anti-HA antibodies, respectively (Fig. S1*A*), whereas MURC-FLAG expression was reduced in the supernatant immunoprecipitated by the anti-HA antibody, although PTRF/Cavin-1-HA expression was not reduced in the supernatant immunoprecipitated by the anti-FLAG antibody (Fig. S1*B*). These results suggest that MURC/Cavin-4 binds to PTRF/Cavin-1 with high affinity, and that MURC/Cavin-3 does not entirely bind to Cav-3.

The bimolecular fluorescence complementation (BiFC) assay confirmed that MURC/Cavin-4, Cav-3, PTRF/Cavin-1, and SDPR/Cavin-2 interact in living cardiomyocytes (Fig. S1 *C* and *D*). Immunoelectron microscopy revealed that MURC/Cavin-4 was expressed in caveolae and T tubules in cardiomyocytes of adult mice (Fig. 1*A*). These observations are in accordance with our previous finding showing that MURC/Cavin-4 was localized to the Z line in cardiomyocytes (11) because the T-tubule system is in register with the Z lines and the immunostaining pattern of Cav-3 has been shown to coincide with the Z line in the heart (19). Because it was confirmed that MURC/Cavin-4 was expressed by caveolae, we assessed whether MURC/Cavin-4 affected caveolar morphology in cardiomyocytes. In cardiomyocytes of 13-wk-old MURC-Tg mice, the caveolae were significantly distended compared with those of wild-type (WT) mice (Fig. 1*B*). The effects of MURC/Cavin-4 on caveolae were supported by the results of an in vitro study in which MURC/Cavin-4 overexpression significantly increased the caveolar area and perimeter in cardiomyocytes compared with β-galactosidase (LacZ) overexpression (Fig. 1*C*). These results indicated that MURC/Cavin-4 modified the morphology of formed caveolae in cardiomyocytes.

MURC/Cavin-4 Is Associated with α1-ARs at Caveolae in Cardiomyocytes. We next investigated the localization of α1-ARs in cardiomyocytes. α1-AR exists as three molecular subtypes: α1A, -B. and -D. The α1A and -B subtypes are expressed in the myocardium, whereas the α1D subtype is expressed in vascular muscle (20). Because antibodies for α1-AR subtypes, which are frequently cited, have been shown to be nonspecific (21), we used plasmids encoding red fluorescent protein mCherry-conjugated α1A-AR (ADRA1A) and α1B-AR (ADRA1B). ADRA1A and ADRA1B signals were observed predominantly at the plasma membrane and partly within the cytoplasm (Fig. 2*A*). ADRA1A and ADRA1B signals were colocalized with endogenous Cav-3 and MURC/Cavin-4 at the plasma membrane and partly within the cytoplasm. Immunoprecipitation and BiFC assays revealed that both ADRA1A and ADRA1B were bound to MURC/Cavin-4 in COS cells and cultured rat cardiomyocytes, respectively (Fig. 2 *B* and *C*).

Because Cav-3 has also been demonstrated to bind to α1-ARs (22), we investigated whether Cav-3 could influence the localization of MURC/Cavin-4 and α1-ARs in cardiomyocytes. Cav-3 knockdown impaired the plasma membrane localization of MURC/Cavin-4, resulting in the accumulation of MURC/Cavin-4 in the cytosol of cardiomyocytes (Fig. S2 *A*–*C*). However, α1-ARs were retained at the plasma membrane in Cav-3–knocked down cardiomyocytes (Fig. S2*A*).

MURC/Cavin-4 Deficiency Attenuates α1-AR–Induced ERK Activation and Cardiac Hypertrophy. The above-mentioned observations that α1-ARs bound to MURC/Cavin-4 at caveolae in cardiomyocytes led us to examine whether MURC/Cavin-4 influenced the response to α1-AR stimulation in vivo. To this end, we subjected WT and

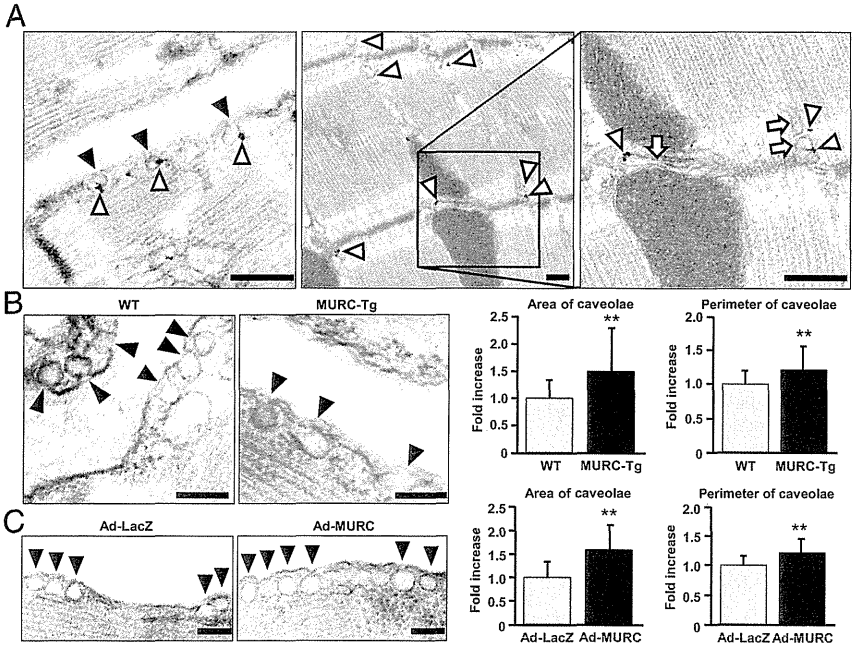

Fig. 1. MURC/Cavin-4 exists in the caveolae and T tubules and modulates caveolar morphology in cardiomyocytes. Representative electron microscopic images of mouse heart tissue and adult cultured cardiomyocytes. (*A*) Immunogold staining of MURC/Cavin-4 (white arrowheads) was observed at caveolae (black arrowheads) and T tubules (white arrows) of cardiomyocytes. (*B* and *C*) Representative shapes of caveolae in mouse heart tissue (*B*, *Left*) and rat cultured cardiomyocytes with or without MURC/Cavin-4 overexpression (*C*, *Left*). Caveolae were identified by their characteristic flask shapes and locations at or near the plasma membrane. Relative caveolar areas and perimeters were measured in cardiomyocytes from heart tissue (*B*, *Right*) and cultured cardiomyocytes (*C*, *Right*). Data are presented as mean ± SEM. $^{**}P < 0.01$ compared with controls. (Scale bars: 500 nm in *A*; and 200 nm in *B* and *C*.)

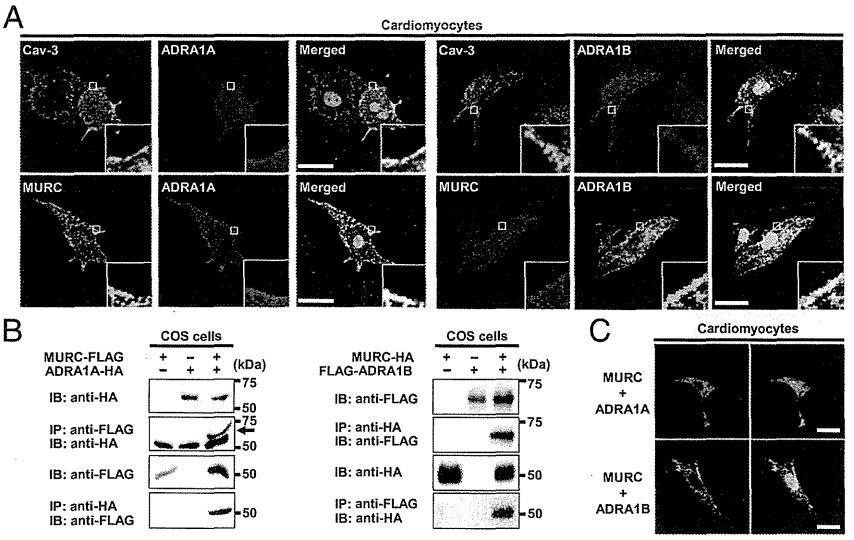

Fig. 2. MURC/Cavin-4 is associated with α1-ARs at caveolae in cardiomyocytes. (*A*) Representative fluorescence images of rat neonatal cardiomyocytes. Cardiomyocytes were cotransfected with ADRA1A- or ADRA1B-pmCherry. MURC/Cavin-4 and Cav-3 were costained with ADRA1A and ADRA1B (white boxes). (*B*) COS cells were transfected with MURC/Cavin-4-FLAG and/or ADRA1A-HA (*Left*), or with MURC/Cavin-4-HA and/or FLAG-ADRA1B (*Right*). The black arrow indicates ADRA1A-HA. (*C*) In situ association of MURC/Cavin-4 with α1-ARs in living cardiomyocytes was confirmed using the BiFC assay. Cardiomyocytes were cotransfected with phmKGC-MN-MURC and phmKGN-MN-ADRA1A or phmKGN-MN-ADRA1B. Nuclei were stained with DAPI (blue). (Scale bars: 20 μm in *A* and *C*.) IB, immunoblots; IP, immunoprecipitation. mKGC, monomeric Kusabira Green.

MURC/Cavin-4–null (*MURC*$^{-/-}$) mice (Fig. S3 *A* and *B*) to α1-AR–induced cardiac hypertrophy. *MURC*$^{-/-}$ mice are fertile, exhibit normal growth under normal conditions (Fig. S3*C*), and are indistinguishable by cardiac mass and function from WT mice under physiological conditions (Tables S1 and S2). Furthermore, caveolae and Cav-3 localization at the plasma membrane are retained in cardiomyocytes of *MURC*$^{-/-}$ mice (Fig. S3 *D* and *E*), indicating that MURC/Cavin-4 is not essential to the membrane localization of Cav-3 and caveola formation in cardiomyocytes. Phenylephrine (PE) infusion for 7 d caused marked concentric cardiac hypertrophy in WT mice, whereas MURC/Cavin-4 depletion suppressed cardiac hypertrophy, as evaluated using a cross-sectional area (Fig. 3*A*). Morphological and echocardiographic analyses also showed attenuated cardiac hypertrophy in *MURC*$^{-/-}$ mice (Tables S1 and S2). In the hearts of *MURC*$^{-/-}$ mice, BNP and βMHC mRNA expression levels were reduced in response to PE, compared with those of WT mice (Fig. 3*B*). A previous study demonstrated that, in ADRA1A and ADRA1B double-knockout (KO) (α1AB-KO) mice, ERK activation was reduced and PE could not activate ERK in cardiomyocytes, resulting in a reduced heart size in α1AB-KO mice compared with that in male WT mice (23). Therefore, we investigated ERK activation in WT and *MURC*$^{-/-}$ hearts. After PE infusion for 2 d, ERK activation was significantly suppressed in the hearts of *MURC*$^{-/-}$ mice compared with WT mice (Fig. 3*C*). In neonatal mouse cardiomyocytes isolated from WT and *MURC*$^{-/-}$ mice, PE-induced ERK activation was also significantly suppressed in *MURC*$^{-/-}$ cardiomyocytes compared with the level in WT cardiomyocytes (Fig. S3*F*). Mitogen-activated protein kinases (MAPKs), including ERK1/2, modulate cardiac hypertrophy through G proteins (24). Therefore, we assessed p38 and JNK activities in the hearts of WT and *MURC*$^{-/-}$ mice (Fig. S3*G*). The basal activity of p38 did not differ between WT and *MURC*$^{-/-}$ hearts, whereas JNK activation was significantly increased in *MURC*$^{-/-}$ hearts compared with the level in WT hearts. However, both p38 and JNK activities were not enhanced by PE infusion in the hearts of WT and *MURC*$^{-/-}$ mice.

MURC/Cavin-4 Serves as an ERK-Recruiting Protein in the Caveolae and Modulates α1-AR–Induced Hypertrophic Responses in Cardiomyocytes. To clarify the molecular mechanisms responsible for MURC/Cavin-4–mediated cardiac hypertrophy, we knocked down MURC expression in neonatal rat cardiomyocytes. PE increased MURC/Cavin-4 mRNA expression in cardiomyocytes, whereas MURC/Cavin-4 RNA interference (RNAi) using Ad-rMURC short hairpin RNA (shRNA) attenuated PE-induced MURC/Cavin-4 mRNA expression (Fig. S4*A*). MURC/Cavin-4 RNAi reduced PE-induced increases in cell size and BNP mRNA expression (Fig. S4 *B* and *C*), which is consistent with the in vivo study described above. PE-induced ERK activation was also suppressed in neonatal rat cardiomyocytes infected with Ad-MURC-shRNA as well as mouse cardiomyocytes isolated from *MURC*$^{-/-}$ mice (Fig. 4*A*). In cardiomyocytes infected with Ad-Luc-shRNA, ERK activation was detected 5 min after PE stimulation, which peaked at 30 min and then declined, whereas in cardiomyocytes infected with Ad-MURC-shRNA, ERK activation peaked at 5 min and then declined, which was significantly suppressed compared with that in Ad-Luc-shRNA–infected cardiomyocytes, suggesting that MURC/Cavin-4 plays a determinant role in the modulation of signaling amplitude and the duration of ERK activation in response to PE stimulation.

A previous study using immunoelectron microscopy showed that ERK was concentrated in caveolae (25). ERK is activated at the plasma membrane by several GPCRs and subsequently translocates to the nucleus and cytoplasm (26). Therefore, we investigated the functional role of MURC/Cavin-4 in ERK localization. In unstimulated cardiomyocytes, total and phosphorylated ERK was distributed throughout the cytoplasm and partially at the plasma membrane, where it was colocalized with MURC (Fig. 4*B*). Upon PE stimulation, both MURC/Cavin-4 and phosphorylated ERK were translocated from the plasma membrane to the perinuclear region (Fig. 4 *B* and *C*). MURC/Cavin-4 knockdown reduced phosphorylated ERK accumulation at the plasma membrane (Fig. 4*D*). Immunoblot analysis showed that MURC/Cavin-4 coimmunoprecipitated with phosphorylated and total ERK (Fig. 4*E*).

The stability of ERK proteins influences the duration of ERK activity (27). Thus, we evaluated the stability of phosphorylated and total ERK using cycloheximide (CHX), a protein biosynthesis inhibitor. The stability of phosphorylated and total ERK proteins was significantly increased following CHX treatment in MURC-expressing cardiomyocytes compared with the level in those expressing LacZ (Fig. S4*D*).

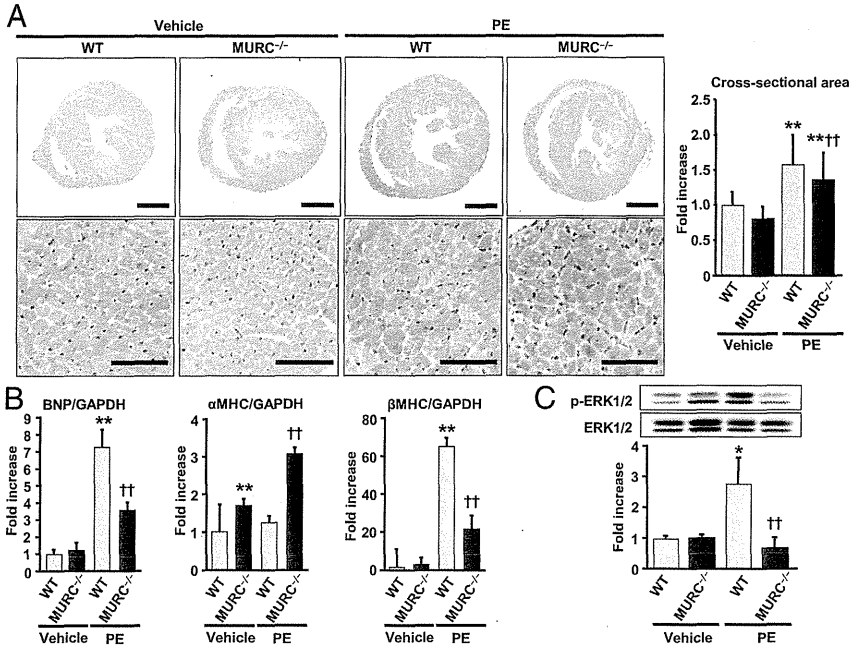

Fig. 3. MURC/Cavin-4 deletion attenuates α1-AR–induced ERK1/2 activation and cardiac hypertrophy. (*A*) Representative H&E staining of WT and *MURC*$^{-/-}$ heart paraffin-embedded sections (*A*, *Upper*, *Left*) and measurement of relative myocyte cross-sectional area (*A*, *Upper*, *Right*). WT and *MURC*$^{-/-}$ mice were infused with PE for 7 d with osmotic minipumps. Higher magnification images are shown (*Lower*). (Scale bars: 1 mm in *Upper*; and 50 μm in *Lower*.) A bar graph showing cross-sectional areas relative to vehicle-treated WT mice. (*B*) Measurements of BNP, αMHC, and βMHC mRNA levels in the heart. (*C*) Measurement of ERK1/2 activation in the heart. WT and *MURC*$^{-/-}$ mice were infused with PE for 2 d with osmotic minipumps. Data are presented as mean ± SEM. $^{*}P < 0.05$ and $^{**}P < 0.01$ compared with vehicle-treated WT mice; $^{\dagger\dagger}P < 0.01$ compared with PE-treated WT mice.

MURC/Cavin-4 Modulates α1-AR–Induced Cardiomyocyte Hypertrophy Through ERK Activation. We previously demonstrated cardiomyocyte hypertrophy in young MURC-Tg mice (11). In the present study, we found that ERK activity was increased in the cardiomyocytes of 6-wk-old MURC-Tg mice (Fig. 5*A*) and that MURC/Cavin-4 overexpression promoted cardiomyocyte hypertrophy (Fig. 5*B*). Furthermore, ERK1/2 siRNA knockdown (Fig. S5) significantly inhibited MURC/Cavin-4- and α1-AR–induced increase in cardiomyocyte size (Fig. 5 *C* and *D*). These results indicated that MURC/Cavin-4 was required for ERK activation in cardiomyocyte hypertrophy. ERK activity is regulated by MEK (28); therefore, to determine whether MURC/Cavin-4 modulates ERK activation through MEK1/2, we measured MEK1/2 activity in cardiomyocytes (Fig. S6). Under basal conditions, MURC/Cavin-4 overexpression did not affect MEK1/2 activation, whereas ERK was activated by MURC/Cavin-4 overexpression compared with LacZ. MEK1/2 activation in MURC/Cavin-4–overexpressing PE-stimulated cardiomyocytes was significantly enhanced compared with that in LacZ-overexpressing cardiomyocytes. In addition, ERK activation was synergistically enhanced by MURC/Cavin-4

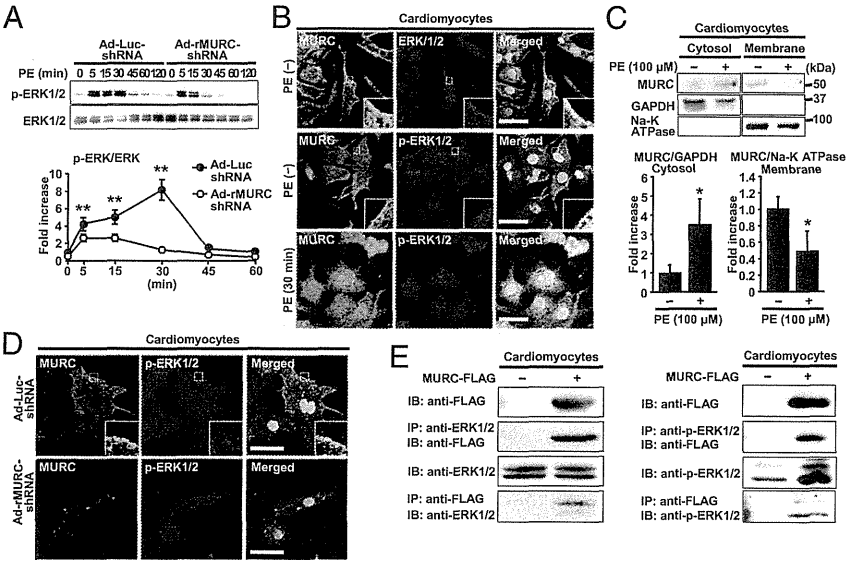

Fig. 4. MURC/Cavin-4 serves as an ERK1/2-recruiting protein in the caveolae and modulates α1-induced hypertrophic responses in cardiomyocytes. (*A*) Representative Western blots (*Upper*) and quantification of ERK phosphorylation (*Lower*) in cardiomyocytes with 100 μM PE. Data are presented as mean ± SEM. $^{**}P < 0.01$ compared with Ad-LucshRNA; $^{\dagger\dagger}P < 0.01$ compared with PE-treated Ad-Luc shRNA. (*B*) Representative immunostaining of ERK1/2 and MURC/Cavin-4 in cardiomyocytes. MURC/Cavin-4 was costained with ERK1/2 and p-ERK1/2 (white boxes). (*C*) Representative Western blots (*Upper*) and quantification of MURC protein levels in the cytosol and membrane fractions (*Lower*). Cells were treated with 100 μM PE for 30 min. (*D*) Representative immunostaining of p-ERK1/2 and MURC in MURC knocked-down cardiomyocytes. (Scale bars: 20 μm in *B* and *D*.) (*E*) Cell lysates were subjected to immunoprecipitation with anti-FLAG, anti-ERK1/2 (*Left*) and anti–p-ERK1/2 (*Right*) antibodies. Nuclei were stained with DAPI (blue).

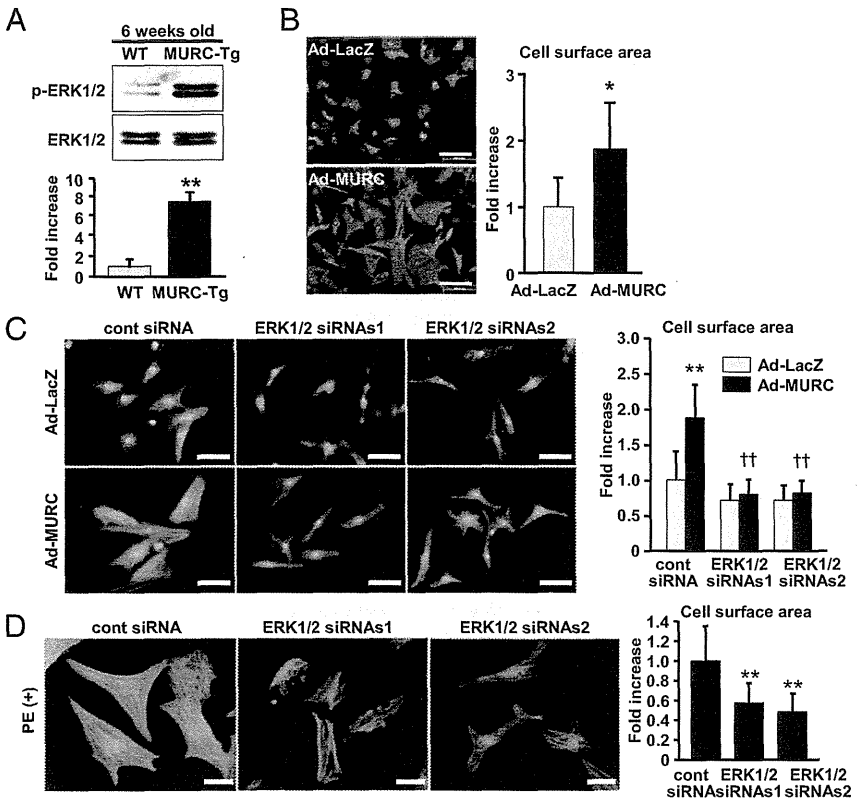

Fig. 5. MURC/Cavin-4 modulates α1-AR–induced cardiomyocyte hypertrophy through ERK1/2 activation. (*A*) Representative Western blots (*Upper*) and quantification of ERK1/2 phosphorylation (*Lower*) in 6-wk-old WT and MURC-Tg mice. $^{**}P < 0.01$ compared with WT mice. (*B*) Representative phalloidin-FITC–stained cardiomyocytes (*Left*) and quantification of cell surface area (*Right*). $^{*}P < 0.05$ compared with Ad-LacZ. (*C*) Representative fluorescence images of cardiomyocytes (*Left*) and quantification of cell surface area (*Right*). $^{**}P < 0.01$ compared with control siRNA-transfected Ad-LacZ; $^{\dagger\dagger}P < 0.01$ compared with control siRNA-transfected Ad-MURC. (*D*) Representative phalloidin-FITC–stained cardiomyocytes stimulated by PE. Cardiomyocytes were transfected with ERK1/2 siRNA and then stimulated by 100 μM PE for 48 h (*Left*), and cell surface area was quantified (*Right*). $^{**}P < 0.01$ compared with control siRNA. (Scale bars: 100 μm in *B*; and 50 μm in *C* and *D*.) All cells were stained by phalloidin-FITC. Nuclei were stained by DAPI (blue). ERK1/2 siRNAs1 indicates ERK1 siRNA-1 and ERK2 siRNA-1 cotransfection, and ERK1/2 siRNAs2 indicates ERK1 siRNA-2 and ERK2 siRNA-2 cotransfection. Data are presented as mean ± SEM.

overexpression in response to PE stimulation. Taken together, these findings suggested that MURC/Cavin-4 was capable of regulating ERK activation in a MEK1/2-dependent and -independent manner and that MURC/Cavin-4 served as a caveolar platform, thereby allowing activated α1-ARs to elicit MEK1/2 activation efficiently.

Discussion

Similar to caveolins, cavins are caveolar components that modulate caveolar morphology (29). Among the cavins, PTRF/Cavin-1 is required for caveola formation in various cell types including epithelium, smooth muscle, and skeletal muscle (16, 30). A recent study showed that SDPR/Cavin-2 deletion caused a pronounced reduction in caveola abundance in lung endothelium, but not in heart endothelium and that SRBC/Cavin-3 deletion did not affect caveolar formation in these cells (31). We demonstrated in the present study that MURC/Cavin-4 modified the morphology of formed caveolae in cardiomyocytes, whereas MURC/Cavin-4 was not essential to caveolar formation. Thus, all cavin proteins do not necessarily have the ability to form caveolae. Cav-3 KO mice showed a loss of caveolae in cardiomyocytes, leading to ERK activation and cardiac hypertrophy (19). We showed that Cav-3 knockdown reduced MURC/Cavin-4 localization at the plasma membrane, whereas MURC/Cavin-4 deficiency did not impair the membrane localization of Cav-3. Furthermore, unlike Cav-3 KO mice, MURC/Cavin-4–deficient mice exhibit normal caveolar morphology and function under physiological conditions. MURC/Cavin-4 deficiency attenuated ERK activation and cardiac hypertrophy induced by α1-AR stimulation. These results indicate that MURC/Cavin-4 regulates ERK activity and cardiac hypertrophy independently of caveolar morphology.

MURC/Cavin-4 bound to ERK1/2 in cardiomyocytes, and MURC/Cavin-4 and phosphorylated ERK were cotranslocated from the plasma membrane to the perinuclear region in response to PE. MURC/Cavin-4 knockdown attenuated PE-induced phosphorylated ERK accumulation at the plasma membrane. These findings suggest that MURC/Cavin-4 interacts with ERK and promotes ERK recruitment to caveolae and subsequent internalization by the caveolae. We also showed that MURC/Cavin-4 increased the stability of phosphorylated and total ERK proteins in cardiomyocytes, which suggests that MURC/Cavin-4 stabilized ERK proteins to prevent their inactivation and/or degradation, thereby sustaining ERK activation. Although scaffold proteins involved in ERK signaling, such as kinase suppressor of Ras (KSR), MAPK kinase (MEK) partner 1, MAPK organizer 1, and β-arrestin, have been identified (32), the relationship between these scaffolds and the caveolae has not been documented. Our results provide the unique documentation that MURC/Cavin-4 is a scaffold protein for ERK in caveolae and contributes to the stabilization of ERK activity in cardiomyocytes. Thus, MURC/Cavin-4 spatiotemporally regulates α1-AR–induced ERK activation in cardiomyocytes.

Several studies have demonstrated that α1-ARs were localized to the plasma membrane (19, 33, 34), whereas Wright et al. (35) showed that α1-ARs were located around or within the nucleus, but not on the plasma membrane, in adult mouse cardiomyocytes. Thus, controversy exists regarding the localization of α1-ARs in cardiomyocytes. Because of a lack of proper antibodies for α1-AR subtypes (21), we expressed fluorescent protein-tagged α1-ARs in cardiomyocytes and showed that α1A- and α1B-ARs were colocalized with MURC/Cavin-4 and Cav-3 at the plasma membrane and partly within the cytoplasm in cardiomyocytes. It has been revealed that many GPCRs form oligomeric complexes, as either homo- or heterooligomers, and that GPCR oligomerization has effects on ligand binding, receptor activation, desensitization, and trafficking, as well as receptor signaling (21). We showed that MURC/Cavin-4 enhanced MEK1/2 activation in response to PE stimulation in cardiomyocytes. Because MURC/Cavin-4 interacts with α1A- and α1B-AR, our observations raise the possibility that MURC/Cavin-4 might contribute to an increase in the accessibility between each of the α1-ARs, which leads to α1-AR oligomerization and promotes α1-AR signaling. A previous

study reported that MEK1 was distributed in caveolae (25). On the basis of this evidence, we predicted that MURC/Cavin-4 interacted with MEK1/2 as well as ERK in the caveolae, although coimmunoprecipitation analysis did not demonstrate an association between MURC/Cavin-4 and MEK1/2. Considering that MURC/Cavin-4 is colocalized with α1-ARs, MURC/Cavin-4 may also contribute to the functional compartmentation of α1-AR signaling of the caveolae, which facilitates the responsiveness of MEK1/2 activation in response to α1-AR stimulation, although MURC/Cavin-4 does not interact with MEK1/2 directly.

In cultured cardiomyocytes, ERK depletion using an antisense oligonucleotide was shown to down-regulate PE-induced hypertrophic responses (36). In the present study, ERK1/2 knockdown inhibited MURC/Cavin-4– and PE-induced cardiomyocyte hypertrophy. Thus, ERK has a crucial role in α1-AR– and MURC/Cavin-4–induced cardiac hypertrophy. Furthermore, MURC/Cavin-4 knockdown inhibited PE-induced cardiomyocyte hypertrophy associated with ERK inactivation. These findings suggested that MURC/Cavin-4 mediated PE-induced ERK signaling in cardiomyocytes.

Although the role of ERK signaling in cardiomyocyte hypertrophy is unknown (37), activated MEK1 induced concentric cardiac hypertrophy with ERK1/2 activation in transgenic mice (28). ERK1/2-deficient mice showed increases in the heart:body weight ratio and reductions in cardiac contractility under physiological conditions, which resulted in eccentric hypertrophy and cardiomyocyte elongation (38). Furthermore, angiotensin II and PE stimulation worsened eccentric cardiac growth in ERK1/2-deficient mice. However, in our present study, 1 wk of PE infusion inhibited concentric hypertrophy in *MURC*$^{-/-}$ mice, but did not promote eccentric hypertrophy, despite the inhibition of ERK activation. The discrepancy between these studies may be explained by a difference in the levels of suppressed ERK activity. Eccentric hypertrophy and cardiomyocyte elongation were observed in ERK1/2-deficient mice, which have complete loss of ERK activity (38). On the other hand, MURC/Cavin-4 deficiency maintained baseline ERK activity in the cardiomyocytes compared with that in control mice under physiological conditions. These observations suggested that concentric hypertrophy was modulated by ERK activation, which is induced by various stimuli, and that eccentric hypertrophy was modulated by a reduction in basal ERK activity.

As shown in the present study, although MURC/Cavin-4 is dispensable for caveolar formation in cardiomyocytes, MURC/Cavin-4 serves as an ERK-recruiting protein in the caveolae within cardiomyocytes. The recruiting function of MURC/Cavin-4 is necessary to elicit efficient signaling of the α1-AR/ERK cascade in the caveolae in concentric cardiac hypertrophy, which provides unique insight into the molecular mechanisms underlying caveola-mediated signaling in cardiac hypertrophy.

Materials and Methods

Pearson product-moment correlation coefficient was used to measure the linear correlation between variables. All experiments were performed at least thrice. Data are expressed as mean ± SEM and were analyzed by one-way ANOVA with post hoc analysis. A P value of <0.05 was considered significant.

The other materials and methods used for this study are described in *SI Materials and Methods*.

ACKNOWLEDGMENTS. We greatly appreciate Dr. H. Kasahara (University of Florida College of Medicine) for valuable suggestions. This work was supported by Grants-in-Aid from the Ministry of Education, Culture, Sports, Science, and Technology of Japan; the Japan Association for the Advancement of Medical Equipment; and the Takeda Science Foundation and the Mitsubishi Pharma Research Foundation.

1. Shaul PW, Anderson RG (1998) Role of plasmalemmal caveolae in signal transduction. *Am J Physiol* 275(5 Pt 1):L843–L851.
2. Parton RG, Simons K (2007) The multiple faces of caveolae. *Nat Rev Mol Cell Biol* 8(3):185–194.
3. Razani B, Woodman SE, Lisanti MP (2002) Caveolae: From cell biology to animal physiology. *Pharmacol Rev* 54(3):431–467.
4. Cohen AW, Hnasko R, Schubert W, Lisanti MP (2004) Role of caveolae and caveolins in health and disease. *Physiol Rev* 84(4):1341–1379.
5. Harvey RD, Calaghan SC (2012) Caveolae create local signalling domains through their distinct protein content, lipid profile and morphology. *J Mol Cell Cardiol* 52(2):366–375.
6. Hansen CG, Nichols BJ (2010) Exploring the caves: Cavins, caveolins and caveolae. *Trends Cell Biol* 20(4):177–186.
7. Briand N, Dugail I, Le Lay S (2011) Cavin proteins: New players in the caveolae field. *Biochimie* 93(1):71–77.
8. Williams TM, Lisanti MP (2004) The Caveolin genes: From cell biology to medicine. *Ann Med* 36(8):584–595.
9. Gratton JP, Bernatchez P, Sessa WC (2004) Caveolae and caveolins in the cardiovascular system. *Circ Res* 94(11):1408–1417.
10. Bastiani M, et al. (2009) MURC/Cavin-4 and cavin family members form tissue-specific caveolar complexes. *J Cell Biol* 185(7):1259–1273.
11. Ogata T, et al. (2008) MURC, a muscle-restricted coiled-coil protein that modulates the Rho/ROCK pathway, induces cardiac dysfunction and conduction disturbance. *Mol Cell Biol* 28(10):3424–3436.
12. Rodriguez G, et al. (2011) Molecular genetic and functional characterization implicate muscle-restricted coiled-coil gene (MURC) as a causal gene for familial dilated cardiomyopathy. *Circ Cardiovasc Genet* 4(4):349–358.
13. McMahon KA, et al. (2009) SRBC/cavin-3 is a caveolin adapter protein that regulates caveolae function. *EMBO J* 28(8):1001–1015.
14. Hayashi YK, et al. (2009) Human PTRF mutations cause secondary deficiency of caveolins resulting in muscular dystrophy with generalized lipodystrophy. *J Clin Invest* 119(9):2623–2633.
15. Bastiani M, Parton RG (2010) Caveolae at a glance. *J Cell Sci* 123(Pt 22):3831–3836.
16. Hill MM, et al. (2008) PTRF-Cavin, a conserved cytoplasmic protein required for caveola formation and function. *Cell* 132(1):113–124.
17. Hansen CG, Bright NA, Howard G, Nichols BJ (2009) SDPR induces membrane curvature and functions in the formation of caveolae. *Nat Cell Biol* 11(7):807–814.
18. Allen JA, Halverson-Tamboli RA, Rasenick MM (2007) Lipid raft microdomains and neurotransmitter signalling. *Nat Rev Neurosci* 8(2):128–140.
19. Woodman SE, et al. (2002) Caveolin-3 knock-out mice develop a progressive cardiomyopathy and show hyperactivation of the p42/44 MAPK cascade. *J Biol Chem* 277(41):38988–38997.
20. Jensen BC, Swigart PM, De Marco T, Hoopes C, Simpson PC (2009) α1-Adrenergic receptor subtypes in nonfailing and failing human myocardium. *Circ Heart Fail* 2(6):654–663.
21. Breitwieser GE (2004) G protein-coupled receptor oligomerization: Implications for G protein activation and cell signaling. *Circ Res* 94(1):17–27.
22. Fujita T, et al. (2001) Accumulation of molecules involved in alpha1-adrenergic signal within caveolae: Caveolin expression and the development of cardiac hypertrophy. *Cardiovasc Res* 51(4):709–716.
23. O'Connell TD, et al. (2003) The $\alpha_{(1A/C)}$- and $\alpha_{(1B)}$-adrenergic receptors are required for physiological cardiac hypertrophy in the double-knockout mouse. *J Clin Invest* 111(11):1783–1791.
24. Muslin AJ (2008) MAPK signalling in cardiovascular health and disease: Molecular mechanisms and therapeutic targets. *Clin Sci (Lond)* 115(7):203–218.
25. Liu P, Ying Y, Anderson RG (1997) Platelet-derived growth factor activates mitogen-activated protein kinase in isolated caveolae. *Proc Natl Acad Sci USA* 94(25):13666–13670.
26. Kholodenko BN, Hancock JF, Kolch W (2010) Signalling ballet in space and time. *Nat Rev Mol Cell Biol* 11(6):414–426.
27. Lu Z, Xu S, Joazeiro C, Cobb MH, Hunter T (2002) The PHD domain of MEKK1 acts as an E3 ubiquitin ligase and mediates ubiquitination and degradation of ERK1/2. *Mol Cell* 9(5):945–956.
28. Bueno OF, et al. (2000) The MEK1-ERK1/2 signaling pathway promotes compensated cardiac hypertrophy in transgenic mice. *EMBO J* 19(23):6341–6350.
29. Nabi IR (2009) Cavin fever: Regulating caveolae. *Nat Cell Biol* 11(7):789–791.
30. Liu L, et al. (2008) Deletion of Cavin/PTRF causes global loss of caveolae, dyslipidemia, and glucose intolerance. *Cell Metab* 8(4):310–317.
31. Hansen CG, Shvets E, Howard G, Riento K, Nichols BJ (2013) Deletion of cavin genes reveals tissue-specific mechanisms for morphogenesis of endothelial caveolae. *Nat Commun* 4:1831.
32. Dhanasekaran DN, Kashef K, Lee CM, Xu H, Reddy EP (2007) Scaffold proteins of MAP-kinase modules. *Oncogene* 26(22):3185–3202.
33. Petrashevskaya NN, Bodi I, Koch SE, Akhter SA, Schwartz A (2004) Effects of α1-adrenergic stimulation on normal and hypertrophied mouse hearts. Relation to caveolin-3 expression. *Cardiovasc Res* 63(3):561–572.
34. Koga A, et al. (2003) Adenovirus-mediated overexpression of caveolin-3 inhibits rat cardiomyocyte hypertrophy. *Hypertension* 42(2):213–219.
35. Wright CD, et al. (2008) Nuclear α1-adrenergic receptors signal activated ERK localization to caveolae in adult cardiac myocytes. *Circ Res* 103(9):992–1000.
36. Glennon PE, et al. (1996) Depletion of mitogen-activated protein kinase using an antisense oligodeoxynucleotide approach downregulates the phenylephrine-induced hypertrophic response in rat cardiac myocytes. *Circ Res* 78(6):954–961.
37. Kehat I, Molkentin JD (2010) Extracellular signal-regulated kinase 1/2 (ERK1/2) signaling in cardiac hypertrophy. *Ann N Y Acad Sci* 1188:96–102.
38. Kehat I, et al. (2011) Extracellular signal-regulated kinases 1 and 2 regulate the balance between eccentric and concentric cardiac growth. *Circ Res* 108(2):176–183.

DOI: 10.1111/joic.12002

STRUCTURAL HEART DISEASE

Long-Term Effects of Transcatheter Closure of Atrial Septal Defect on Cardiac Remodeling and Exercise Capacity in Patients Older than 40 Years with a Reduction in Cardiopulmonary Function

YOICHI TAKAYA, M.D.,[1] MANABU TANIGUCHI, M.D.,[2,3] TEIJI AKAGI, M.D.,[2] SAORI NOBUSADA, M.T.,[4] KENGO KUSANO, M.D.,[1] HIROSHI ITO, M.D.,[1] and SHUNJI SANO, M.D.,[2,5]

From the [1]Department of Cardiovascular Medicine, Okayama University Graduate School of Medicine, Dentistry and Pharmaceutical Sciences, Okayama, Japan; [2]Division of Cardiac Intensive Care Unit, Okayama University Hospital, Okayama, Japan; [3]Division of Cardiovascular Medicine, Fukuyama Cardiovascular Hospital, Fukuyama, Japan; [4]Division of Central Clinical Laboratory, Okayama University Hospital, Okayama, Japan; and [5]Department of Cardiovascular Surgery, Okayama University Graduate School of Medicine, Dentistry and Pharmaceutical Sciences, Okayama, Japan

Background: *Although it has been demonstrated that cardiac remodeling and exercise capacity improve after transcatheter closure of atrial septal defect (ASD), little is known about long-term benefits in middle-aged and elderly patients with a reduction in cardiopulmonary function.*
Objectives: *To evaluate long-term extent and time course of improvements in cardiac remodeling and exercise capacity in those patients.*
Methods: *Twenty ASD patients ≥ 40 years of age with a reduction in cardiopulmonary function (predicted peak oxygen uptake [VO_2] < 65%) were enrolled. Transthoracic echocardiography and cardiopulmonary exercise testing were performed at baseline and at 1 month, 3 months, 6 months, and >12 months after the procedure.*
Results: *At 1 month after the procedure, significant decreases in right ventricular (RV) end-diastolic diameter (38.2 ± 4.4 to 31.9 ± 4.4 mm; P < 0.001) and RV/left ventricular end-diastolic diameter ratio (0.95 ± 0.17 to 0.71 ± 0.13; P < 0.001) occurred, and they were maintained during the follow-up period. Normal RV size was achieved in 11 of 18 patients with RV enlargement. Predicted peak VO_2 did not change at 1 month and 3 months, but it improved significantly after 6 months (53.6 ± 6.5 to 62.1 ± 12.6%; P < 0.01). Sixteen of the 20 patients showed improved predicted peak VO_2.*
Conclusions: *Cardiac remodeling and exercise capacity could be improved over the long-term period after transcatheter closure of ASD in middle-aged and elderly patients with a reduction in cardiopulmonary function. There were differences in the time course of improvement between cardiac remodeling and exercise capacity in those patients.* (J Interven Cardiol 2013;26:195–199)

Introduction

Atrial septal defect (ASD) of secundum type is one of the most common forms of congenital heart disease in adults. Many patients with ASD are usually asymptomatic in early life, but clinical symptoms such as fatigue and dyspnea develop frequently in the course of time.[1,2] The development of clinical symptoms, echocardiographic signs of shunt volume or shunt-related pulmonary hypertension are widely accepted indications for closure of ASD. It is well known that surgical closure of ASD leads to long-term functional benefits in middle-aged and elderly symptomatic patients.[3–6] In recent years, transcatheter closure of ASD has been established as a secure and effective treatment, and it has become an important alternative to surgical repair for ASD.[7,8] A few studies

Conflict of interest: None

Address for reprints: Manabu Taniguchi, M.D., 2–39 Midorimachi, Fukuyama-shi, Hiroshima 720-0804, Japan. Fax: +81-84-925-9650; e-mail: tmnb@hotmail.com

have shown short-term benefits of transcatheter closure of ASD on cardiac remodeling and exercise capacity in middle-aged and elderly patients.[9,10] However, little is known about long-term results. Furthermore, the extent and time course of functional improvements after the procedure in middle-aged and elderly patients with a marked reduction in cardiopulmonary function remains unclear. Therefore, the aim of this study was to investigate the long-term extent and time course of improvements in cardiac remodeling and exercise capacity after transcatheter closure of ASD in those patients.

Methods

Study Population. From June 2006 to April 2009, 20 consecutive ASD patients $\geq$ 40 years of age with a moderate or severe reduction in cardiopulmonary function who underwent transcatheter closure of secundum ASD were enrolled. We defined moderate reduction in cardiopulmonary function as 50% $\leq$ predicted peak oxygen uptake (VO_2) < 65%, and we defined severe reduction as predicted peak VO_2 < 50%. The indications for ASD closure in all patients were significant left-to-right shunt detected by echocardiography, presence of right ventricular (RV) volume overload, shunt-related symptoms, or pulmonary hypertension. Exclusion criteria included pulmonary vascular resistance > 8 wood units on 100% O_2 and transesophageal maximal ASD diameter > 40 mm. The Okayama University Ethics Committee approved this study, which was performed in accordance with the Helsinki declaration, and all patients provided written informed consent before participation in this study.

Transcatheter Closure of ASD. Transesophageal echocardiography was performed in all patients before the procedure, and left atrial thrombi were not detected in any of the patients. Coronary angiography was performed in all patients, and there was no significant coronary stenosis. Transcatheter closure of ASD using an AMPLATZER septal occluder device (AGA Medical Corporation; Plymouth, MN, USA) was performed under general anesthesia with the assistance of transesophageal echocardiography. Hemodynamic evaluation was performed just before ASD closure. With oxygen uptake measured at rest, the pulmonary to systemic flow ratio was calculated by oxymetry using the Fick principle. If the pulmonary wedge pressure increased > 5 mmHg from baseline, the procedure was abandoned.

Echocardiography. Transthoracic echocardiography was performed at baseline and at 1 month, 3 months, 6 months, and >12 months after the procedure using a 3.5 MHz transducer (Aplio, Toshiba, Otawara, Japan). Left ventricular (LV) end-diastolic diameter, LV end-systolic diameter, and RV end-diastolic diameter were measured by M-mode parasternal echocardiography, and RV/LV end-diastolic diameter ratio was calculated. LV ejection fraction was derived using Teichholz's formula. These measurements were done at least three times and averaged to obtain mean values by 2 independent experienced investigators who were blinded to the data of treatment.

Cardiopulmonary Exercise Testing. Cardiopulmonary exercise testing was performed at baseline and at 1 month, 3 months, 6 months, and >12 months after the procedure. All patients underwent symptom-limited exercise tests on an upright bicycle ergometer using a ramp protocol (15 W/min) with simultaneous respirator gas analysis. Patients were encouraged to exercise to exhaustion or to a respiratory exchange ratio $\geq$ 1.09. Blood pressure and heart rate were measured every minute. A 12-lead electrocardiogram was continuously monitored during exercise testing. Breathed gas was continuously collected to analyze VO_2, carbon dioxide production, and minute ventilation with a gas analyzer. Peak VO_2 was defined as the highest VO_2 value achieved at peak exercise after reaching the respiratory compensation point, and predicted peak VO_2 was expressed according to age, sex, weight, and height. VO_2 to work rate ratio ($\Delta VO_2/\Delta WR$) was determined. A spirometric measurement was performed to assess vital capacity and forced expiratory volume in 1 second. These analyses were done by 2 independent experienced investigators who were blinded to the data of treatment.

Statistical Analysis. Variables are expressed as means $\pm$ standard deviation or percentage. Statistical analysis was performed by Wilcoxon's matched-pairs test. A P value < 0.05 was considered to be statistically significant.

Results

Study Population. Patient clinical characteristics are summarized in Table 1. Mean age at transcatheter closure of ASD was 54.5 $\pm$ 10.9 years (range, 40–78 years). Fourteen patients (70%) were female. ASD diameter measured by transesophageal echocardiography was 17.8 $\pm$ 4.3 mm. Pulmonary to

Table 1. Patient Clinical Characteristics

Variables	
Age (years)	54.5 ± 10.9
Female (%)	70
Smoking (%)	25
Lung disease (%)	15
Hypertension (%)	25
Diabetes mellitus (%)	10
Stroke (%)	5
Atrial septal defect diameter (mm)	17.8 ± 4.3
Device size (mm)	21.7 ± 4.7
Pulmonary to systemic flow ratio	2.6 ± 0.6
Mean pulmonary artery pressure (mmHg)	14.5 ± 4.0
Vital capacity (l)	2.9 ± 0.6
Forced expiratory volume in 1 second (l/second)	2.3 ± 0.6

Data are presented as mean ± standard deviation or percentage.

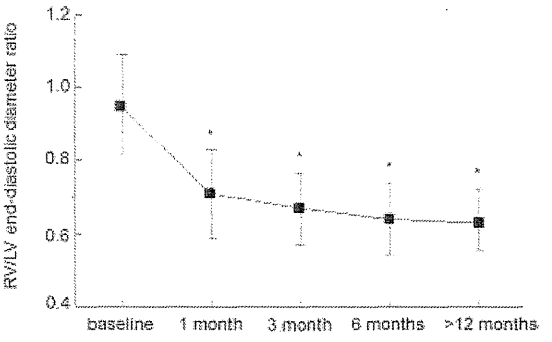

Figure 1. Time course of data on RV/LV end-diastolic diameter after transcatheter closure of atrial septal defect. *P < 0.001 versus baseline. RV = right ventricular; LV = left ventricular.

systemic flow ratio was 2.6 ± 0.6, and mean pulmonary artery pressure under general anesthesia was 14.5 ± 4.0 mmHg. Transcatheter closure of ASD was performed successfully in all patients using an AMPLATZER septal occluder device. All patients were followed up for a mean period of 25.2 ± 10.5 months (range, 12.0–40.8 months). There were no complications including thromboembolic events in the procedural and follow-up period.

Cardiac Remodeling and Exercise Capacity. Time courses of data obtained by transthoracic echocardiography and cardiopulmonary exercise testing at baseline and after the procedure are summarized in Table 2. At baseline, RV enlargement (RV end-diastolic diameter >30 mm) was present in 18 patients (90%). After the procedure, a significant decrease in RV end-diastolic diameter was observed at 1 month, and it was maintained during the follow-up period. Eleven of 18 patients with RV enlargement (61%) achieved a normal RV size (RV end-diastolic diameter <30 mm). In addition, LV end-diastolic diameter increased significantly. Therefore, cardiac remodeling resulted in a decrease in RV/LV end-diastolic diameter ratio at 1 month (Fig. 1). LV ejection fraction and LV end-systolic diameter did not change from baseline. At baseline, 13 patients (65%) had a moderate reduction in cardiopulmonary function and 7 patients (35%) had a severe reduction. After the procedure, predicted peak VO_2 did not change at 1 month and 3 months, but it improved significantly after 6 months (Fig. 2). Predicted peak VO_2 increased overall by 15%, and 16 of the 20 patients (80%), including 10 of the 13 patients with a moderate reduction in cardiopulmonary function and 6 of the 7 patients with a severe reduction in cardiopulmonary function, showed improved predicted peak VO_2 in the follow-up period. In addition, a

Table 2. Transthoracic Echocardiography and Cardiopulmonary Exercise Testing at Baseline and After Transcatheter Closure of Atrial Septal Defect

Variables	Baseline	1 month	3 months	6 months	>12 months
LV end-diastolic diameter (mm)	40.7 ± 5.0	45.7 ± 5.3**	46.1 ± 4.7**	46.5 ± 5.3**	46.6 ± 5.2***
LV end-systolic diameter (mm)	24.4 ± 3.9	26.9 ± 3.7	26.2 ± 3.1	26.8 ± 3.9	26.8 ± 3.6
LV ejection fraction (%)	71.2 ± 5.2	72.3 ± 4.0	74.0 ± 4.4	73.4 ± 5.4	73.6 ± 4.7
RV end-diastolic diameter (mm)	38.2 ± 4.4	31.9 ± 4.4***	30.5 ± 3.5***	29.6 ± 3.2***	29.3 ± 2.9***
RV/LV end-diastolic diameter ratio	0.95 ± 0.17	0.71 ± 0.13***	0.67 ± 0.10***	0.64 ± 0.10***	0.63 ± 0.08***
Predicted peak oxygen uptake (%)	53.6 ± 6.5	55.8 ± 11.5	56.8 ± 9.7	62.1 ± 12.6**	61.8 ± 9.7**
Peak oxygen uptake (ml/min/kg)	15.4 ± 2.3	16.3 ± 3.7	16.0 ± 2.9	17.6 ± 3.9*	17.5 ± 3.5*
Oxygen uptake to work rate ratio	7.3 ± 1.8	6.9 ± 1.6	7.9 ± 1.6	8.1 ± 1.7	8.3 ± 1.4*

Data are presented as mean ± standard deviation.
*P < 0.05 versus baseline, ** P < 0.01 versus baseline, *** P < 0.001 versus baseline.
LV = left ventricular; RV = right ventricular.

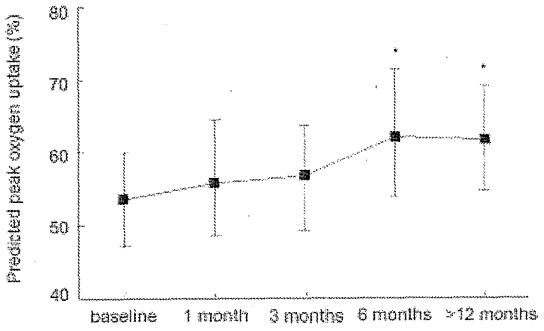

Figure 2. Time course of data on predicted peak oxygen uptake after transcatheter closure of atrial septal defect. *P < 0.01 versus baseline.

significant improvement in $\Delta VO_2/\Delta WR$ was observed at > 12 months after the procedure.

Discussion

In this study, we evaluated long-term functional benefits of transcatheter closure of ASD in middle-aged and elderly patients with a marked reduction in cardiopulmonary function, and we found significant improvements in cardiac remodeling and exercise capacity. Decrease or even normalization of RV size and RV/LV end-diastolic diameter ratio occurred early after the procedure, and they were maintained during the long-term period. Exercise capacity measured by cardiopulmonary exercise testing did not change early, but it improved during the long-term period. We also found the time delay of improvement in exercise capacity compared with cardiac remodeling in those patients. The severity of functional limitation increases with advancing age in the majority of patients with ASD.[1,2] The clinical courses and long-term results after surgery depend mainly on the patient's preoperative clinical status. In the past, controversy existed as to whether middle-aged and elderly patients benefit from surgery. Murphy et al.[11] proved that symptomatic patients who undergo surgery after the age of 40 years were at increased risk for postoperative cardiovascular complications, whereas young adults had an excellent prognosis. However, several studies have demonstrated long-term benefits of surgical ASD closure in middle-aged and elderly symptomatic patients.[3–6] Konstantinides et al.[3] showed that surgical ASD closure in symptomatic patients over the age of 40 years increased long-term survival and prevented deterioration of New York Heart Association (NYHA) functional class during a follow-up period of 8.9 years. Jemielity et al.[4], in patients aged 40–62 years and followed for 6.9 years, also found a significant improvement in functional class with 61.8% patients in NYHA functional class III and IV before surgery compared with 82.4% in NYHA functional class I and II after surgery. These studies indicated that surgical ASD closure benefits many or most middle-aged and elderly symptomatic patients in the long-term period and therefore it is widely recommended for those patients. Recently, transcatheter closure of ASD has been performed safely and effectively, and it has become an alternative to surgical ASD closure.[7,8] Similar to surgical repair, several studies have demonstrated functional benefits of transcatheter closure of ASD in adult patients.[12–15] Giardini et al.[12] evaluated long-term impacts of transcatheter closure of ASD on RV remodeling and exercise capacity in asymptomatic patients, and they found a significant decrease in RV diameter and a significant improvement in peak VO_2. In comparison with this study, their study population was younger and had less severe cardiopulmonary function at the time of the procedure. Our study population consisted of only patients ≥ 40 years of age with a marked reduction in cardiopulmonary function to investigate patients considered at higher risk for functional recovery after the procedure. Regarding middle-aged and elderly patients, Brochu et al.[9] investigated results in asymptomatic or mildly symptomatic patients over the age of 40 years, and they showed that peak VO_2 was increased significantly at 6 months after the procedure. Jategaonkar et al.[10] reported a significant decrease in RV end-diastolic diameter and significant improvements of NYHA functional class and peak VO_2 at 3 months after the procedure even in patients over the age of 60 years. However, little is known about long-term results in those patients. Furthermore, although impaired exercise capacity is a predictive parameter in terms of mortality in congenital heart disease,[16,17] limited information is available for long-term extent of functional improvement in middle-aged and elderly patients with markedly reduced cardiopulmonary function. The recently published study of Khan et al.[18] showed significant improvements in cardiac remodeling and 6-min walk test at 12 months after the procedure in patients over the age of 40 years. Our results are similar to their findings. However, we also evaluated the time course of functional improvements, and we revealed that an improvement in exercise capacity was delayed compared with cardiac remodeling in middle-aged and elderly patients with a marked reduction in cardiopulmonary function. The mechanism leading to improved exercise capacity after the

procedure has been clarified. ASD closure with abolishment of left-to-right shunt leads to augmented LV filling by increased preload and therefore to improved stroke volume.[14] The rise in cardiac output may explain the increase of exercise capacity. In this study, we found the time delay of improvement in exercise capacity compared with cardiac remodeling. In addition, even if RV size was normalized in more than half of all patients, mean exercise capacity continued to be at least moderately reduced. Exercise capacity is influenced by several factors, not only cardiac output but also noncardiac factors such as pulmonary function and skeletal muscle function. We speculated that the delay of improvement in exercise capacity could be related to the time needed for the recover of skeletal muscle function after transcatheter closure of ASD in middle-aged and elderly patients with a marked reduction in cardiopulmonary function, but not the time needed for the recover of cardiac function. Similar to our results, Helber et al.[19] showed the lack of improvement in exercise capacity early after surgical ASD closure in patients over the age of 40 years, and they suggested that the improvement in exercise capacity took place after 1–2 years after the procedure. Thus, exercise training after the procedure may be needed to recover the pulmonary function and skeletal muscle function early in those patients.

Study Limitations. This study had some limitations. First, the current findings need confirmation in large studies because this study included only 20 patients from a single center. Second, exercise capacity is also influenced by noncardiac factors, but measurements of those factors are lacking. Finally, the evaluation of RV function using two-dimensional strain echocardiography, three-dimensional echocardiography, or tricuspid annular plane systolic excursion should be preferable to demonstrate RV remodeling after transcatheter closure of ASD.

Conclusion

Transcatheter closure of ASD in patients $\geq$ 40 years of age with markedly reduced cardiopulmonary function resulted in significant long-term improvements of cardiac remodeling and functional capacity. There were differences in the time course of improvement between cardiac remodeling and exercise capacity after the procedure in those patients.

References

1. Fredriksen PM, Veldtman G, Hechter S, et al. Aerobic capacity in adults with various congenital heart disease. Am J Cardiol 2001;87:310–314.
2. Markmann P, Howitt G, Wade EG. Atrial septal defect in the middle-aged and elderly. Quant J Med 1965;34:409–426.
3. Konstantinides S, Geibel A, Olschewski M, et al. A comparison of surgical and medical therapy for atrial septal defect in adults. N Engl J Med 1995;333:469–473.
4. Jemielity M, Dyszkiewicz W, Paluszkiewicz L, et al. Do patients over 40 years of age benefit from surgical closure of atrial septal defects? Heart 2001;85:300–303.
5. Nasrallah AT, Hall RJ, Garcia E, et al. Surgical repair of atrial septal defect in patients over 60 years of age. Long-term results. Circulation 1976;53:329–331.
6. Sutton MG, Tajik AJ, McGoon DC. Atrial septal defect in patients aged 60 years or older: Results and long-term postoperative follow-up. Circulation 1981;64:402–409.
7. Masura J, Gavora P, Formanek A, et al. Transcatheter closure of secundum atrial septal defects using the new self-centering amplatzer septal occluder: Initial human experience. Cathet Cardiovasc Diagn 1997;42:388–393.
8. Masura J, Gavora P, Podnar T. Long-term outcome of transcatheter secundum-type atrial septal defect closure using Amplatzer septal occluders. J Am Coll Cardiol 2005;45:505–507.
9. Brochu MC, Baril JF, Dore A, et al. Improvement in exercise capacity in asymptomatic and mildly symptomatic adults after atrial septal defect percutaneous closure. Circulation 2002;106:1821–1826.
10. Jategaonkar S, Scholtz W, Schmidt H, et al. Percutaneous closure of atrial septal defects: Echocardiographic and functional results in patients older than 60 years. Circ Cardiovasc Interv 2009;2:85–89.
11. Murphy JG, Gersh BJ, McGoon MD, et al. Long term outcome after surgery repair of isolated atrial septal defects. Follow-up at 27 to 32 years. N Engl J Med 1990;323:1645–1650.
12. Giardini A, Donti A, Specchia S, et al. Long-term impact of transcatheter atrial septal defect closure in adults on cardiac function and exercise capacity. Int J Cardiol 2008;124:179–182.
13. Veldtman GR, Razack V, Siu S, et al. Right ventricular form and function after percutaneous atrial septal defect device closure. J Am Coll Cardiol 2001;37:2108–2113.
14. Giardini A, Donti A, Formigari R, et al. Determinants of cardiopulmonary function improvement after transcatheter atrial septal defect closure in asymptomatic adults. J Am Coll Cardiol 2004;43:1886–1891.
15. Schoen SP, Kittner T, Bohl S, et al. Transcatheter closure of atrial septal defects improves right ventricular volume, mass, function, pulmonary pressure, and functional class: A magnetic resonance imaging study. Heart 2006;92:821–826.
16. Diller GP, Dimopoulos K, Okonko D, et al. Exercise intolerance in adult congenital heart disease: Comparative severity, correlates, and prognostic implication. Circulation 2005;112:828–835.
17. Giardini A, Specchia S, Berton E, et al. Strong and independent prognostic value of peak circulatory power in adults with congenital heart disease. Heart 2007;154:441–447.
18. Khan AA, Tan JL, Li W, et al. The impact of transcatheter atrial septal defect closure in the older population: A prospective study. JACC Cardiovasc Interv 2010;3:276–281.
19. Helber U, Baumann R, Seboldt H, et al. Atrial septal defect in adults: Cardiopulmonary exercise capacity before and 4 months and 10 years after defect closure. J Am Coll Cardiol 1997;29:1345–1350.

Artificial
Organs

Guest Editorial

Outcomes of the Ninth International Conference on Pediatric Mechanical Circulatory Support Systems and Pediatric Cardiopulmonary Perfusion

The Ninth International Conference on Pediatric Mechanical Circulatory Support Systems and Pediatric Cardiopulmonary Perfusion was held at the Hershey Lodge in Hershey, PA, USA from May 8 to 11, 2013.

The overall objective of this annual conference remains to bring together internationally known clinicians, bioengineers, and basic scientists involved in research on pediatric mechanical circulatory support (MCS) systems and pediatric cardiopulmonary bypass (CPB) procedures. The main focus is to explicitly describe the problems with current pediatric MCS systems, methods, and techniques during acute and chronic support, and to suggest solutions and future directions for research. During the past 9 years, the main focus has not changed but has given the highest possible educational opportunities to the diverse participants. More hands-on wet labs and simulations with the newest devices and techniques have been added (1,2).

JOHN A. WALDHAUSEN, MD

The Ninth International Conference was dedicated in honor and memory of John A. Waldhausen, MD, Professor Emeritus, for his life-long contributions as the Founding Chair of the Department of Surgery at Pennsylvania State University College of Medicine (PSUCOM) and as a pioneering surgeon and educator in the development of pediatric cardiac surgery in the USA (Fig. 1).

CONFERENCE PROGRAM

John L. Myers, MD, and Professor Emeritus William S. Pierce, MD, of PSUCOM presented remarks in remembrance of Dr. Waldhausen on the opening day of the conference (Fig. 2). After these opening remarks, we asked if anyone in the audience would like to share any memories of Dr. Waldhausen with the participants. One of the legends of MCS, Jack G. Copeland, MD, surgeon and inventor, shared his story that Dr. Waldhausen was in fact a chair on his General Surgery Board Oral Examination and let Dr. Copeland know that he passed the test after he answered his challenging questions.

This year, conference attendees had the opportunity to hear two keynote lectures during the morning session on Thursday, May 9, the first day of the scientific program. The first keynote, presented by Jeffrey Towbin, MD, was entitled "Pediatric Heart Failure Etiologies and the Outcomes of Children with Mechanical Circulatory Support." The second keynote, presented by Shunji Sano, MD, PhD, was entitled "Stem Cell Therapy in Children with HLHS." Both lectures were highly informative and provided excellent insights to the future of MCS (Fig. 3).

Plenary sessions were held throughout the morning and afternoon sessions on Thursday, Friday, and Saturday. The topics of these sessions included "Pediatric MCS: 2013 Update" (moderated by Shunji Sano, MD, PhD, and Jeffrey Towbin, MD), "Neuromonitoring/Neuroprotection during CPB" (moderated by Erle H. Austin III, MD, J. Brian Clark, MD, and Gioanni Battista Luciani, MD), "ECLS Systems: 2013 Update" (moderated by Emre Belli, MD, and Chitra Ravishankar, MD), and "Pediatric Perfusion: 2013 Update" (moderated by Larry Baer, CCP, and Tami Rosenthal, BS, CCP, MBA). The conference also included three minisymposiums on the following topics: "Pediatric Extracorporeal Life Support: Nursing Perspective" (moderated by Paula Baldridge, MSN, MHA, RN and Bonnie Weaver, RN, MSN, CCRN, CCNS), "Bioengineering Approaches in Pediatric Cardiovascular Medicine" (moderated by Kerem Pekkan, PhD, and Jeffrey D. Zahn, PhD), and "Penn State Hershey Pediatric Cardiovascular Research Center—International Collaborations: 2013 Update" (moderated by Akif Ündar, PhD). Oral

doi:10.1111/aor.12213

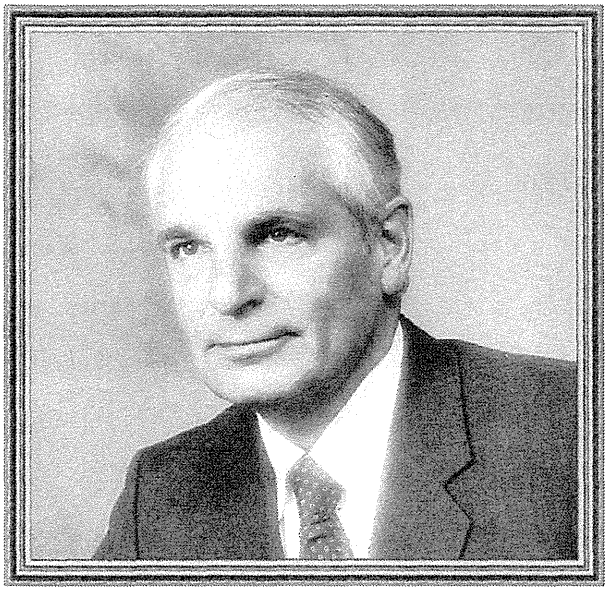

FIG. 1. John A. Waldhausen, MD (1929–2012).

presentations were held in the afternoon sessions on Friday and Saturday. Poster presentations were displayed throughout the duration of the conference.

PEDIATRIC EXTRACORPOREAL LIFE SUPPORT (ECLS) WORKSHOP

As a new feature, the Ninth Conference included a hands-on experience with the newest pediatric ECLS systems (3–6). This session was conducted at the Animal Research Farm on the grounds of PSUCOM during the preconference program on Wednesday, May 8 (Fig. 4). The instructors for this session were Larry Baer, CCP, David Palanzo, CCP, Bonnie Weaver, RN, MSN, CCRN, CCNS, Shigang Wang, MD, Karl Woitas, CCP, J. Brian Clark, MD, Ronald Wilson, VMD, and Akif Ündar, PhD. This session was limited to only 25 participants (nine US centers along with five overseas centers including France, Germany, Italy, Taiwan, and Turkey).

CARDIAC ICU/PICU AND PENN STATE CHILDREN'S HOSPITAL TOURS

In addition to the ECLS workshop, attendees had the opportunity to tour the Cardiac Intensive Care Unit (ICU)/Pediatric Intensive Care Unit (PICU) and the recently opened Penn State Hershey Children's Hospital. The tours of the Cardiac ICU and PICU were led by Penn State Children's Hospital staff and were interactive, allowing active discussion regarding all aspects of patient management and outcomes.

WINE AND CHEESE RECEPTION AT THE HERSHEY STORY

At the conclusion of the scientific program on Friday, attendees were given a 30-min trolley tour of "the sweetest place on earth" by Hershey Trolley Works. Following the tour, attendees participated in a wine and cheese reception at The Hershey Story, the newest museum in Hershey dedicated to the life and legacy of Milton S. Hershey. In addition to the five permanent exhibits on display at the museum, attendees were also able to explore the museum's unique Chocolate Lab, complete with hands-on experiences and interactive demonstrations. In keeping with the musical entertainment provided at previous conferences, attendees were treated to the musical talents of vocalist Heidi Watts, guitarist Tim Vallati, and saxophonist Emre Belli, MD, who again shared his considerable talents with us as he did during the eighth conference (Fig. 5). It was a wonderful evening of wine, cheese, music, chocolate, and conversation.

CONFERENCE AWARDS

This event continues to recognize young investigators, residents, and medical and bioengineering students for their contributions to the advancement of cardiopulmonary bypass and MCS systems for pediatric patients (Fig. 6). This year, three conference awardees were selected for recognition based on their full manuscripts (Table 1). This year, we also repeated a new award called Special Travel Award. Mosthafa Moosa, MD, from New Zealand received the second travel award for traveling the longest distance to attend the conference.

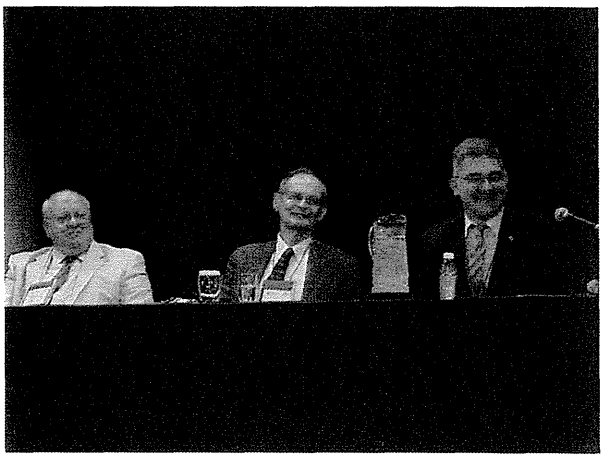

FIG. 2. John L. Myers, MD, Professor Emeritus William S. Pierce, MD, and Akif Ündar, PhD (left to right).

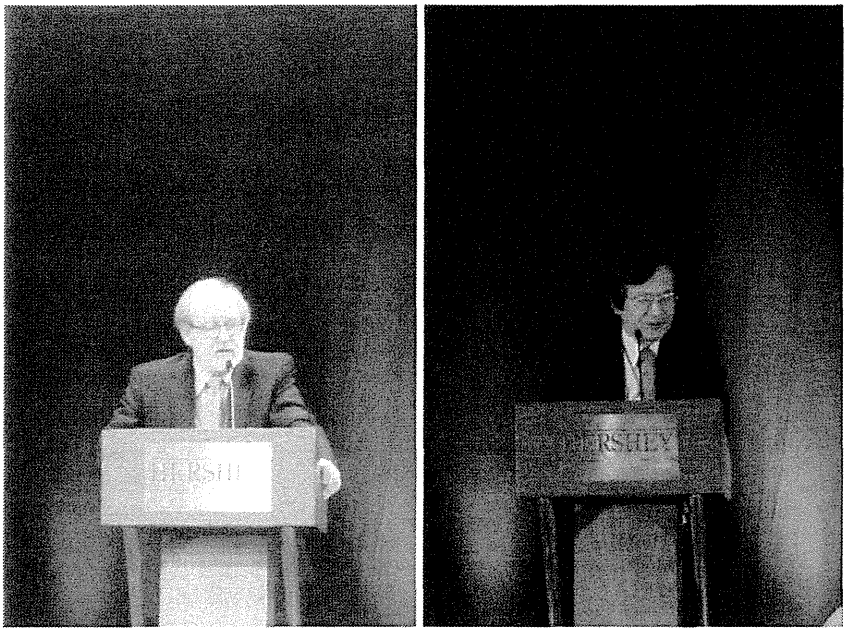

FIG. 3. The keynote lecturers Jeffrey Towbin, MD, and Shunji Sano, MD, PhD.

ARTIFICIAL ORGANS

As in the past, all of the accepted conference abstracts for the Ninth Conference were published in the May 2013 issue of the peer-reviewed journal *Artificial Organs*. In addition, the January 2014 issue of *Artificial Organs* (this issue) is dedicated to peer-reviewed manuscripts that were based on regular slide and poster presentations during the conference. Special thanks to Carol Malchesky, Editorial Assistant, Angela T. Hadsell, Executive Editor, and Paul S. Malchesky, DEng, Editor-in-Chief, for making this special issue possible and for their continued support year after year.

To date, over 400 manuscripts, including original articles, editorials, special reports, and case reports have been peer-reviewed and published in *Artificial Organs*. These publications have become the largest resource for investigators in their research projects related to pediatric CPB and MCS.

Artificial Organs has the highest impact factor compared with all artificial organs journals and is

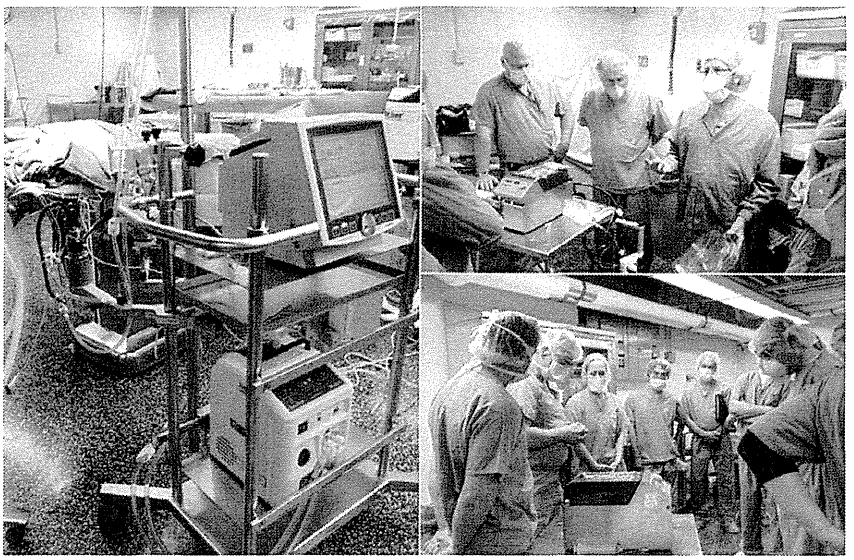

FIG. 4. Hands-on experience with the newest pediatric ECLS systems at the Animal Research Farm on the grounds of PSUCOM.

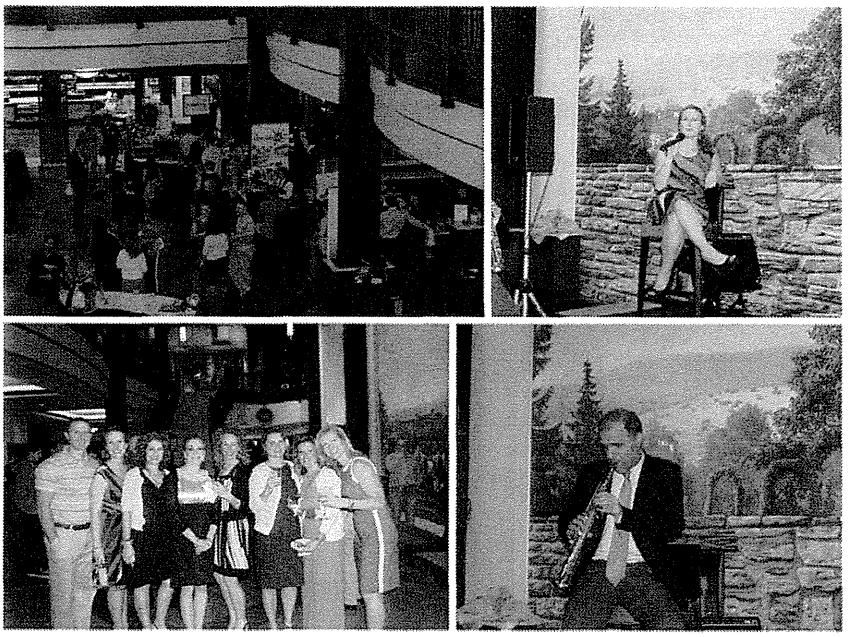

FIG. 5. A wonderful evening of wine, cheese, music, chocolate, and conversation at The Hershey Story.

FIG. 6. Young investigator awardees, clockwise from the top left: Conrad Krawiec, Sertaç Haydin, Hyoung Woo Chang, and Musthafa Moosa.

TABLE 1. *Ninth International Conference Awards*

Award	Awardee	Title of Manuscript
John A. Waldhausen, MD, Young Investigator Award	Conrad Krawiec, MD	Impact of pulsatile flow on hemodynamic energy in a Medos Deltastream DP3 pediatric extracorporeal life support system
William S. Pierce, MD, Young Investigator Award	Hyoung Woo Chang, MD	Five-year experience with mini-volume priming in infants <5 kg: Safety of significantly less transfusion volume
Aydin Aytaç, MD, Young Investigator Award	Sertaç Haydin, MD	Initial experiences with Medos Deltastream DP3 pediatric extracorporeal life support system
Special Travel Award	Musthafa Moosa, MD	For travelling the longest distance for the attendance of conference

now the official journal of the International Society for Pediatric Mechanical Cardiopulmonary Support (7).

FINANCIAL SUPPORT

This year, we are proud to say we received educational support and funds from the International Society for Pediatric Mechanical Cardiopulmonary Support. Although this unique society was only established in 2010 during the Sixth International Conference in Boston, it covered over 97% of all expenses for the Ninth International Conference.

Dr. Ündar also contributed from his personal funds to balance the budget during the past three events.

In addition, financial support was received from companies including Medos Medizintechnik AG (Germany)—Platinum level supporter; Covidien, Inc. (USA), Maquet Medical Systems (USA), Syncardia Systems, Inc. (USA), Terumo Cardiovascular Systems (USA), and Wiley Blackwell (USA)—Bronze level supporters.

EDUCATIONAL CREDITS

The Ninth International Conference was approved for the following educational credits: 24.5 American Medical Association Physician's Recognition Award Category 1 Continuing Medical Education (CME) credits, 34.5 Category 1 Continuing Education Unit hours by the American Board of Cardiovascular Perfusion, and 24.6 Category 1 Continuing Education Unit hours by the California Board of Registered Nursing. These very valuable educational credits demonstrate the high quality scientific program we provide year after year.

SUMMARY

Once again, our annual conference was an overwhelming success. We are encouraged by the volume of scholarly work published as a result of our conference, and we look forward to continuing to provide opportunities for the leading investigators in CPB and MCS systems to share their research and encourage further studies to improve the lives of pediatric patients. To date, a total of 870 presentations have been made at our conferences, and over 400 peer-reviewed articles have been published based on the conference proceedings. All of the details regarding the Ninth International Conference, as well as the previous eight events and information on future events, can be found at our conference website: http://pennstatehershey.org/web/pedscpb/home. As we prepare for the Tenth International Conference in 2014, we continue to set our sights on the goal of publishing over 500 peer-reviewed manuscripts and having over 1000 presentations in the first 10 years of our conference.

Acknowledgments: We would specifically like to thank Bonnie Weaver, MSN, RN, for leading the pre-conference events, including the tours of the Cardiac Care/ICU facilities and the new Penn State Children's Hospital. Additionally, Tami Rosenthal, BS, CCP, MBA, and David Palanzo, CCP, are to be thanked for the time they spent selecting and organizing the new pediatric devices used in the hands-on ECLS workshop. In addition, we sincerely appreciate all the conference organizational support we receive from the Pediatric Clinical Research Office at Penn State Hershey. Special thanks go to Heather Stokes, Jennifer Stokes, Erlee Meyers, Jessica Beiler, Julie Vallati, Amy Shelly, Gabrielle H. Murray, and Shigang Wang, MD, of the Pediatric Cardiovascular Research Center at Penn State Hershey who were instrumental in organizing this event from start to finish. We also appreciate Ann Hagan's invaluable help organizing CME from the Department of Continuing Medical Education of The Children's Hospital of Philadelphia.

Akif Ündar, PhD,[1] Shigang Wang, MD,[1]
David Palanzo, CCP,[1] Bonnie Weaver, RN, CCRN,[1]
Kerem Pekkan, PhD,[2] Mehmet Agirbasli, MD,[3]
Jeffrey D. Zahn, PhD,[4] Giovanni B. Luciani, MD,[5]

J. Brian Clark, MD,[1] Ronald P. Wilson, VMD,[1] Allen R. Kunselman, MA,[1] Shunji Sano, MD, PhD,[6] Emre Belli, MD,[7] William S. Pierce, MD,[1] and John L. Myers, MD[1]

[1]Penn State Hershey Pediatric Cardiovascular Research Center, Department of Pediatrics, Surgery and Bioengineering, Penn State Hershey College of Medicine, Penn State Hershey Children's Hospital, Hershey, PA, USA; [2]Carnegie Mellon University Biomedical Engineering Department, Pittsburgh PA, USA; [3]Marmara University Medical Center, Department of Cardiology, Istanbul, Turkey; [4]Rutgers, The State University of New Jersey, Bioengineering Department, Piscataway, NJ, USA; [5]University of Verona, Division of Cardiac Surgery, Verona, Italy, [6]Okayama University, Department of Cardiovascular Surgery, Okayama, Japan, [7]Marie Lanneleongue Children's Hospital, Department of Cardiac Surgery, Le Plessis-Robinson, France

REFERENCES

1. Ündar A. Welcome to the 9th International Conference on Pediatric Mechanical Circulatory Support Systems & Pediatric Cardiopulmonary Perfusion. *Artif Organs* 2013;4: 354–6.
2. Ündar A, Akçevin A, Alkan-Bozkaya T, et al. Outcomes of the eighth international conference on pediatric mechanical circulatory support systems and pediatric cardiopulmonary perfusion [Guest Editorial]. *Artif Organs* 2013;37:1–9.
3. Wang S, Kunselman AR, Ündar A. Novel pulsatile diagonal pump for pediatric extracorporeal life support system. *Artif Organs* 2013;37:37–47.
4. Krawiec C, Wang S, Kunselman AR, Ündar A. Impact of pulsatile flow on hemodynamic energy in a Medos Deltastream DP3 pediatric extracorporeal life support system. *Artif Organs* 2014;1:19–27.
5. Wang S, Kunselman AR, Ündar A. In vitro performance analysis of novel pulsatile diagonal pump in simulated pediatric mechanical circulatory support system. *Artif Organs* 2014 (in press).
6. Wang S, Ündar A. Current devices for pediatric extracorporeal life support and mechanical circulatory support systems in the United States [Invited Review]. *Biomed Mater Eng* 2013;23:57–62.
7. Malchesky PS. International Society for Pediatric Mechanical Cardiopulmonary Support selects Artifical Organs as its official journal [Editorial]. *Artif Organs* 2013;37:115.

Catheterization and Cardiovascular Interventions 81:837–842 (2013)

Usefulness of Balloon Angioplasty for the Right Ventricle-Pulmonary Artery Shunt with the Modified Norwood Procedure

Naoki Ohno,[1] MD, Shinichi Ohtsuki,[1*] MD, PhD, Koichi Kataoka,[1] MD, PhD, Kenji Baba,[1] MD, PhD, Yoshio Okamoto,[1] MD, Maiko Kondo,[1] MD, Shunji Sano,[2] MD, PhD, Shingo Kasahara,[2] MD, PhD, Osami Honjo,[2] MD, PhD, and Tsuneo Morishima,[1] MD, PhD

Objective: We sought to evaluate the efficacy of balloon angioplasty (BA) for severely desaturated patients due to a stenotic right ventricle (RV) to pulmonary artery (PA) shunt following modified Norwood procedure. **Methods:** Of 87 patients who underwent a Norwood procedure with the RV-PA shunt between February 1998 through March 2010, 22 (25%) patients underwent BA. The efficacy of BA was assessed by angiographic measurement of the changes in the internal diameters of the stenotic portions of the shunt, changes in arterial saturation and clinical outcomes. **Results:** BA was performed for stenotic RV-PA shunts following stage I palliation (n = 17, 77%), or those placed as an additional blood source (n = 5, 23%, 3 patients awaiting biventricular repair, 2 patients following stage II palliation). The location of the BA was at the distal anastomosis in 12 (54.5%), proximal anastomosis in 21 (95.4%) and in the mid-portion of the shunt in 11 (50%) cases. The diameters of these three shunt portions were measured from the anterior–posterior and lateral angiographic images, increasing significantly after BA ($p < 0.0001$) in all. Arterial saturation significantly improved after BA in all cases (66.5 ± 4.3% to 79.4 ± 3.4%, $p < 0.0001$). Freedom from reintervention was 100%. All patients underwent subsequent elective planned surgery at an appropriate age with no mortality. **Conclusions:** A BA-alone strategy for a stenotic RV-PA shunt was effective for all three shunt portions, minimizing shunt-related premature surgical intervention.

Key words: balloon angioplasty; rv-pa shunt; hypoplastic left heart syndrome; Norwood

BACKGROUND

Since Norwood and colleagues described neonatal open-heart palliation for patients with hypoplastic left heart syndrome (HLHS) [1], the clinical outcome of this procedure has improved dramatically [2,3]. One recent modification, the use of a right ventricle (RV)-to-pulmonary artery (PA) shunt instead of a modified Blalock-Taussig (BT) shunt in stage I palliation, appears to offer more stable hemodynamics by avoiding diastolic run off [4]. A recent randomized trial comparing the two shunt types for stage I palliation showed a significantly higher 1-year transplant-free survival in patients with the RV-PA shunt than those with a BT shunt [5]. However, it also revealed a significantly higher requirement for reintervention in the RV-PA shunt group prior to stage II palliation compared to the BT shunt group [5].

Early stenosis of the RV-PA shunt following stage I palliation has been a well-documented phenomenon [6–10]. The mechanisms of stenosis include kinking or compression of the shunt, distal anastomotic stenosis

[1]Department of Pediatrics, Okayama University Graduate School of Medicine, Dentistry and Pharmaceutical Sciences, Okayama, Japan
[2]Department of Cardiovascular Surgery, Okayama University Graduate School of Medicine, Dentistry and Pharmaceutical Sciences, Okayama, Japan

Conflict of interest: Nothing to report.

*Correspondence to: Shinichi Ohtsuki, MD, PhD, Department of Pediatrics, Okayama University Graduate School of Medicine, Dentistry and Pharmaceutical Sciences, 2-5-1 Shikata-cho, Kita-ku, Okayama-City, Okayama 700-8558, Japan. E-mail: tsuki33@cc.okayama-u.ac.jp

Received 15 March 2012; Revision accepted 17 July 2012

DOI 10.1002/ccd.24576
Published online 17 September 2012 in Wiley Online Library (wileyonlinelibrary.com)

with or without branch PA stenosis, proximal stenosis related to muscular growth or endothelial growth within the shunt lumen. As such, progressive desaturation between stages mandates either early conversion to bidirectional Glenn (BDG) anastomosis or catheter intervention to a stenotic RV-PA shunt. Although there are a few case studies describing the efficacy of stent placement in the RV-PA shunt [6,11–14], limited data exist regarding efficacy and durability of balloon angioplasty (BA) alone. In this study, we reviewed our institutional experiences of BA on the RV-PA shunt focusing on the effectiveness of the procedure, reintervention and subsequent timing of stage II palliation.

SUBJECTS AND MATERIALS

Between February 1998 to March 2010, 87 infants underwent the Norwood procedure with a RV-PA shunt at Okayama University Hospital. The subjects of this study were 22 (25.2%) of the 87 patients who had RV-PA conduit stenosis and severe desaturation.

Surgical Techniques and Institutional Policy

The technique of modified Norwood procedure with a RV-PA shunt has been described elsewhere [4,15]. Briefly, the RV-PA shunt [expanded polytetrafluoroethylene (ePTFE), Gore-Tex, W.L Gore & Associates, Flangstaff, AZ] was created with a distal cuff to minimize the distal anastomotic stenosis and/or branch PA stenosis. All shunts were anastomosed to the stump of the central branch PA, which was inserted into the left side of the reconstructed aorta. A 5 mm ePTFE was used in the majority (20/22 patients, 90%), and 6 mm shunt was used in two patients. In seven cases with excessive pulmonary blood flow, a hemoclip was placed on the RV-PA shunt to restrict the pulmonary blood flow either intraoperatively or at the time of delayed chest closure. The Norwood procedure was used as initial palliation for potential biventricular repair in three patients and at stage II palliation, the RV-PA shunt was left in place providing an additional pulmonary blood flow in 17 patients.

Our institutional policy is to perform stage II palliation at 6 months of age with a body weight of more than 5 kg. Therefore, we used a strategy to treat severely desaturated patients following stage I palliation with a BA. Indications for BA were severe desaturation (arterial saturation less than 70%) clearly related to a RV-PA shunt stenosis. The patients with severe desaturation were investigated by echocardiography [α10 (ALOKA), Vivid 7 (GE Yokogawa Medical Systems), IE33 (PHILIPS)]. Presence of stenosis was evaluated by morphology and flow velocity near and inside the shunt.

Catheterization Techniques

All procedures were performed under general anesthesia. Measurement of the PA pressure was often not performed as the patients were unstable. Biplane angiography was performed using either an INTEGRIS BH5000 (PHILIPS) or Infinix Celeve-I INFX-8000V (TOSHIBA) angiographic system. Several different balloons were used including Wanda, Sasuga, Sterling (Boston Scientific, Natic, MA, USA) or Lacross (GOODMAN CO., LTD, Gifu, Japan) of 5 or 6 mm in diameter and 15–40 mm in lengths. A 5 mm balloon was used in the 5 mm ePTFE shunts, while a 6 mm balloon used in the two 6 mm shunts. The RV-PA shunt was approached from the femoral vein in all cases. A 4-French Judkins right coronary catheter was used to cannulate the conduit, a 0.014"-0.018" inch guide wire was then placed in one of the PA branches. The balloon was inserted into the shunt as quickly as possible and inflated. Multiple inflations were often performed until the waist of the balloon at the stenotic site disappeared. Subsequent effectiveness of BA was evaluated based on increase in the internal diameter of the shunt on the post-BA angiogram and also an increase in the arterial saturation. Imaging was performed again after BA and the diameter of the stenotic portion was measured. Typical images for each of three portions, before and after BA are shown in Fig. 1.

Angiographic Evaluation

The image analysis software Elk C. View version 1.7 (Elk) was used for measurement of the diameter of the stenotic portions. All original angiographic images were retrospectively analyzed off line. Sites of stenosis were divided into 3 groups: RV-PA shunt connection to the central branch PA (distal portion), site of RV-PA shunt connection to the RV (proximal portion), and inside the RV-PA shunt (inside portion). The angiograms were obtained in the anterior-posterior (AP) and lateral projections, with the children in isocenter for magnification correction. The diameter of the stenotic portion was measured independently and compared before and after BA.

Clinical Evaluation

We analyzed data regarding age at the time of BA, body weight, changes in arterial saturation before and after BA, and subsequent postoperative course including time to the next operation.

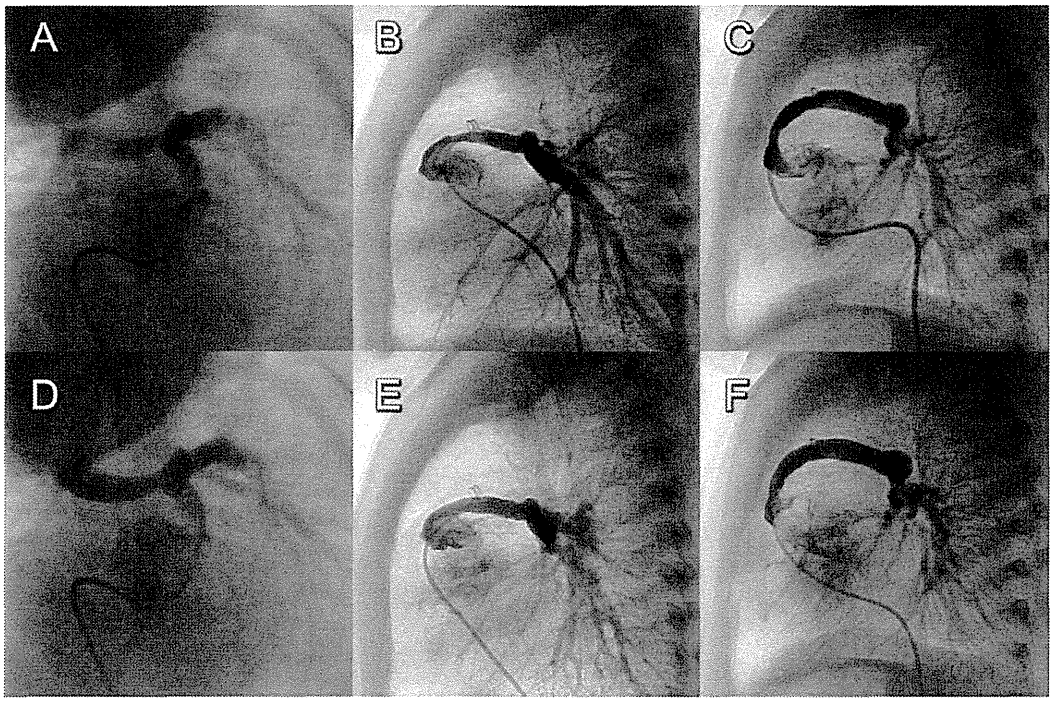

Fig. 1. Figure shows the typical images for each of three portions, before and after BA. A: Distal portion, pre BA, B: Proximal portion pre BA, C: In-stent pre BA, D: Distal portion, post BA, E: Proximal portion, post BA, F: In-stent, post BA.

Statistical Analysis

SPSS II (IBM, United States) was used for statistical analyses. A paired T test was used for comparison of data before and after BA and $p < 0.05$ was considered statistically significant.

RESULTS

Patient Characteristics

Seventeen patients (77%) underwent BA following stage I palliation for single ventricle palliation. The mean age and body weight was 137 days and 4.9 kg, respectively. Five patients had the RV-PA shunt as an additional source of pulmonary blood flow: three awaiting biventricular repair in whom a BT shunt (4 mm) had already been placed and two patients following stage II palliation. The mean age and mean weight of these patients was 547 days and 7.7 kg, respectively.

Efficacy of Balloon Angioplasty

BA was performed at the distal anastomosis in 12 (54.5%), at the proximal anastomosis in 21 (95.4%) and inside the RV-PA shunt in 11 (50%) cases. Eighteen (82%) patients had multiple stenoses. Of 11 patients who underwent BA for the stenosis inside the shunt, seven had a previous hemoclip placed at stage I palliation. The mean fluoroscopy and total procedure times were 28 and 173 min, respectively.

The internal diameters of the RV-PA shunts increased significantly after BA in all three portions ($p < 0.0001$ for all) (Fig. 2). In all cases, arterial saturation also significantly improved (66.5 ± 4.3% to 79.4 ± 3.4%, $p < 0.0001$). During the procedure, transient arrhythmias occurred in two cases with no hemodynamic compromise. There were no other complications during the procedures.

Clinical Outcomes

All 17 patients who underwent BA following stage I palliation had a stable arterial saturation (75.6 ± 2.5%) with favorable weight gain. None of the patients required further catheterization or surgical intervention and underwent an elective BDG with no mortality. The mean age and body weight at surgery was 198 days and 5.6 kg, respectively. Six out of 17 patients completed a TCPC and the remaining 11 patients are awaiting a TCPC completion with no late mortality.

Among the five patients who had an RV-PA shunt as an additional source of pulmonary blood flow, subsequent biventricular repair was performed in three

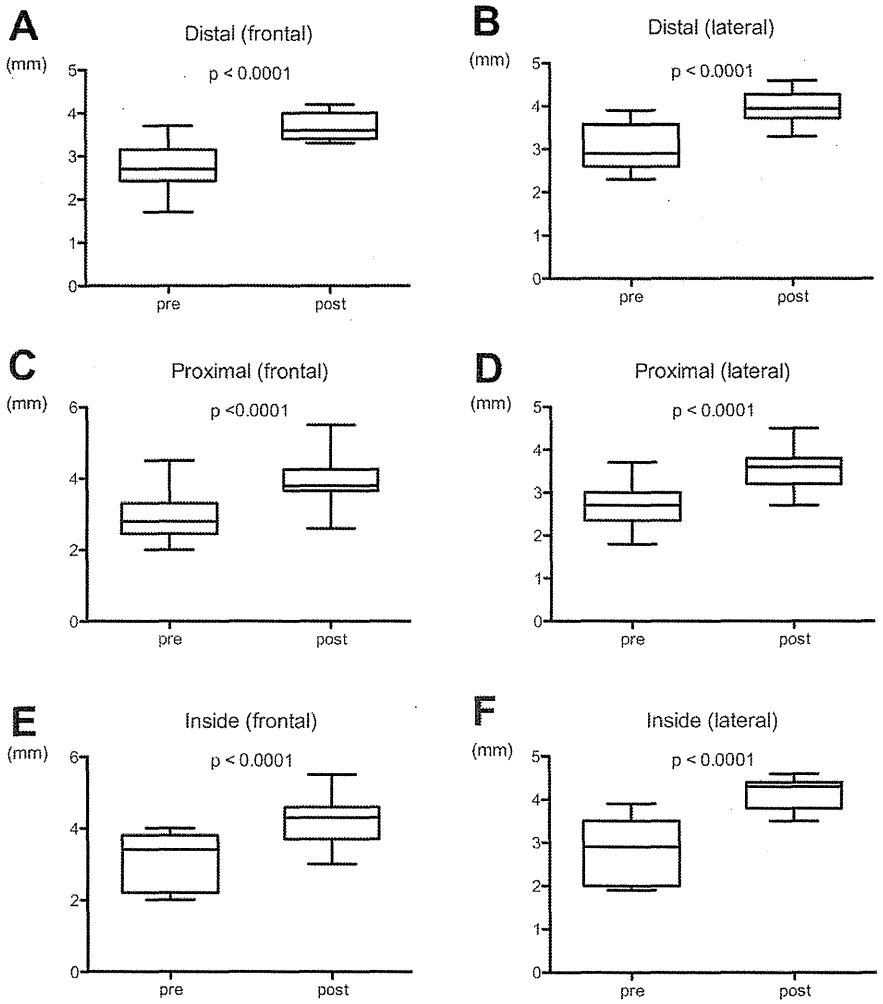

Fig. 2. The changes in the internal diameters before and after BAP. A: Comparison of distal portion in the AP image (2.7 ± 0.6 vs. 3.7 ± 0.3 mm), B: Comparison of distal portion in the lateral image (3.0 ± 0.6 vs. 4.0 ± 0.4 mm), C: Comparison of proximal portion in the AP image (2.9 ± 0.6 vs. 4.0 ± 0.6 mm), D Comparison of proximal portion in the lateral image (2.7 ± 0.5 vs. 3.6 ± 0.4 mm), E Comparison of inside portion in the AP image (3.1 ± 0.8 vs. 4.2 ± 0.7 mm), F Comparison of inside portion in the lateral image (2.9 ± 0.7 vs. 4.1 ± 0.4 mm).

with no mortality with preoperative arterial saturations of 74.3 ± 2.5%. Of the two patients who underwent BA following a BDG, one patient underwent TCPC completion (arterial saturation 78% and body weight 11 kg at the age of 4 years) and the other patient is awaiting TCPC completion (arterial saturation 77%). As a whole, none of the patients experienced desaturation episodes after BA (freedom from reintervention, 100%).

DISCUSSION

Early stenosis of the RV-PA shunt following the modified Norwood procedure is a critical factor contributing to inter-stage mortality and morbidity [3,5]. Progressive desaturation during this period necessitates urgent intervention to re-establish adequate pulmonary blood flow in order to avoid a premature second stage procedure. Our results clearly show that BA was effective in dilating all three portions of stenosis without major complications. Arterial saturations increased significantly and remained stable through the next planned surgical intervention, despite having no stent placed within the shunts. In addition, this strategy worked well for three different clinical situations, i.e., following stage I palliation, an RV-PA shunt as additional pulmonary blood source following stage II palliation and for those having future biventricular repairs.